OPTIMISTIC EXPLORATION WITH BACKWARD BOOTSTRAPPED BONUS FOR DEEP REINFORCEMENT LEARNING

Anonymous authors
Paper under double-blind review

ABSTRACT

Optimism in the face of uncertainty is a principled approach for provably efficient exploration for reinforcement learning in tabular and linear settings. However, such an approach is challenging in developing practical exploration algorithms for Deep Reinforcement Learning (DRL). To address this problem, we propose an Optimistic Exploration algorithm with Backward Bootstrapped Bonus (OEB3) for DRL by following these two principles. OEB3 is built on bootstrapped deep Q-learning, a non-parametric posterior sampling method for temporally-extended exploration. Based on such a temporally-extended exploration, we construct an UCB-bonus indicating the uncertainty of Q-functions. The UCB-bonus is further utilized to estimate an optimistic Q-value, which encourages the agent to explore the scarcely visited states and actions to reduce uncertainty. In the estimation of Q-function, we adopt an episodic backward update strategy to propagate the future uncertainty to the estimated Q-function consistently. Extensive evaluations show that OEB3 outperforms several state-of-the-art exploration approaches in Mnist maze and 49 Atari games.

1 INTRODUCTION

In Reinforcement learning (RL) (Sutton & Barto, 2018) formalized by the Markov decision process (MDP), an agent aims to maximize the long-term reward by interacting with the unknown environment. The agent takes actions according to the knowledge of experiences, which leads to the fundamental problem of the exploration-exploitation dilemma. An agent may choose the best decision given current information or acquire more information by exploring the poorly understood states and actions. Exploring the environment may sacrifice immediate rewards but potentially improves future performance. The exploration strategy is crucial for the RL agent to find the optimal policy.

The theoretical RL offers various provably efficient exploration methods in tabular and linear MDPs with the basic value iteration algorithm: least-squares value iteration (LSVI). *Optimism in the face of uncertainty* (Auer & Ortner, 2007; Jin et al., 2018) is a principled approach. In tabular cases, the optimism-based methods incorporate upper confidence bound (UCB) into the value functions as bonuses and attain the optimal worst-case regret (Azar et al., 2017; Jaksch et al., 2010; Dann & Brunskill, 2015). Randomized value function based on posterior sampling chooses actions according to the randomly sampled statistically plausible value functions and is known to achieve near-optimal worst-case and Bayesian regrets (Osband & Van Roy, 2017; Russo, 2019). Recently, the theoretical analyses in tabular cases are extended to linear MDP where the transition and the reward function are assumed to be linear. In linear cases, optimistic LSVI (Jin et al., 2020) attains a near-optimal worst-case regret by using a designed bonus, which is provably efficient. Randomized LSVI (Zanette et al., 2020) also attains a near-optimal worst-case regret.

Although the analyses in tabular and linear cases provide attractive approaches for efficient exploration, these principles are still challenging in developing a practical exploration algorithm for Deep Reinforcement Learning (DRL) (Mnih et al., 2015; Fujimoto et al., 2018), which achieves human-level performance in large-scale tasks such as Atari games (Machado et al., 2018) and robotic tasks (Andrychowicz et al., 2020). For example, in linear cases, the bonus in optimistic LSVI (Jin et al., 2020) and nontrivial noise in randomized LSVI (Zanette et al., 2020) are tailored to linear

models (Abbasi-Yadkori et al., 2011), and are incompatible with practically powerful function approximations such as neural networks.

To address this problem, we propose the Optimistic Exploration algorithm with Backward Bootstrapped Bonus (OEB3) for DRL. OEB3 is an instantiation of optimistic LSVI (Jin et al., 2020) in DRL by using a general-purpose UCB-bonus to provide an optimistic Q-value and a randomized value function to perform temporally-extended exploration. We propose an UCB-bonus that represents the disagreement of bootstrapped Q-functions (Osband et al., 2016) to measure the epistemic uncertainty of the unknown optimal value function. Q-value added by UCB-bonus becomes an optimistic Q^+ function that is higher than Q for scarcely visited state-action pairs and remains close to Q for frequently visited ones. The optimistic Q^+ function encourages the agent to explore the states and actions with high UCB-bonuses, signifying scarcely visited areas or meaningful events in completing a task. We propose an extension of episodic backward update (Lee et al., 2019) to propagate the future uncertainty to the estimated action-value function consistently within an episode. The backward update also enables OEB3 to perform highly sample-efficient training.

Comparing to existing count-based and curiosity-driven exploration methods (Taiga et al., 2020), OEB3 has several benefits. (1) We utilize intrinsic rewards to produce optimistic value function and also take advantage of bootstrapped Q-learning to perform temporally-consistent exploration while existing methods do not combine these two principles. (2) The UCB-bonus measures the disagreement of Q-values, which considers the long-term uncertainty in an episode rather than the single-step uncertainty used in most bonus-based methods (Pathak et al., 2019; Burda et al., 2019b). Meanwhile, the UCB-bonus is computed without introducing additional modules compared to bootstrapped DQN. (3) We provide a theoretical analysis showing that OEB3 has theoretical consistency with optimistic LSVI in linear cases. (4) Extensive evaluations show that OEB3 outperforms several state-of-the-art exploration approaches in Mnist maze and 49 Atari games.

2 Background

In this section, we introduce bootstrapped DQN (Osband et al., 2016), which we utilize in OEB3 for temporarily-extended exploration. We further introduce optimistic LSVI (Jin et al., 2020), which we instantiate via DRL and propose OEB3.

2.1 Bootstrapped DQN

We consider an episodic MDP represented as $(\mathcal{S}, \mathcal{A}, T, \mathbb{P}, r)$, where $T \in \mathbb{Z}_+$ is the episode length, $\mathcal{S}$ is the state space, $\mathcal{A}$ is the action space, r is the reward function, and $\mathbb{P}$ is the unknown dynamics. In each timestep, the agent obtains the current state s_t, takes an action a_t, interacts with the environment, receives a reward r_t, and updates to the next state s_{t+1}. The action-value function $Q^\pi(s_t, a_t) := \mathbb{E}_\pi\big[\sum_{i=t}^{T-1} \gamma^{i-t} r_i\big]$ represents the expected cumulative reward starting from state s_t, taking action a_t, and thereafter following policy $\pi(a_t|s_t)$ until the end of the episode. $\gamma \in [0, 1)$ is the discount factor. The optimal value function $Q^* = \max_\pi Q^\pi$, and the optimal action $a^* = \arg\max_{a\in\mathcal{A}} Q^*(s, a)$.

Deep Q-Network (DQN) uses a deep neural network with parameters θ to approximate the Q-function. The loss function takes the form of $L(\theta) = \mathbb{E}[(y_t - Q(s_t, a_t; \theta))^2 \big| (s_t, a_t, r_t, s_{t+1}) \sim \mathcal{D}]$, where $y_t = r_t + \gamma \max_{a'} Q(s_{t+1}, a'; \theta^-)$ is the target value, and θ^- is the parameter of the target network. The agent accumulates experiences (s_t, a_t, r_t, s_{t+1}) in a replay buffer $\mathcal{D}$ and samples mini-batches in training.

Bootstrapped DQN (Osband et al., 2016; 2018) is a non-parametric posterior sampling method, which maintains K estimations of Q-values to represent the posterior distribution of the randomized value function. Bootstrapped DQN uses a multi-head network that contains a shared convolution network and K heads. Each head defines a Q^k-function. Bootstrapped DQN diversifies different Q^k by using different random initialization and individual target networks. The loss for training Q^k is

$$L(\theta^k) = \mathbb{E}\Big[\big(r_t + \gamma \max_{a'} Q^k(s_{t+1}, a'; \theta^{k-}) - Q^k(s_t, a_t; \theta^k)\big)^2 \Big| (s_t, a_t, r_t, s_{t+1}) \sim \mathcal{D}\Big]. \quad (1)$$

The k-th head $Q^k(s, a; \theta^k)$ is trained with its own target network $Q^k(s, a; \theta^{k-})$. If k-th head is sampled at the start of an episode when interacting with the environment, the agent will follow Q^k to choose actions in the whole episode, which provides temporally-consistent exploration for DRL.

Algorithm 1 Optimistic LSVI in linear MDP

1: **Initialize:** $\Lambda_t \leftarrow \lambda \cdot \mathbf{I}$ and $w_h \leftarrow 0$
2: **for** episode $m = 0$ **to** $M - 1$ **do**
3: Receive the initial state s_0
4: **for** step $t = 0$ **to** $T - 1$ **do**
5: Take action $a_t = \arg\max_{a \in \mathcal{A}} Q_t(s_t, a)$ and observe s_{t+1}.
6: **end for**
7: **for** step $t = T - 1$ **to** 0 **do**
8: $\Lambda_t \leftarrow \sum_{\tau=0}^{m} \phi(x_t^\tau, a_t^\tau)\phi(x_t^\tau, a_t^\tau)^\top + \lambda \cdot \mathbf{I}$
9: $w_t \leftarrow \Lambda_t^{-1} \sum_{\tau=0}^{m} \phi(x_t^\tau, a_t^\tau)[r_t(x_t^\tau, a_t^\tau) + \max_a Q_{t+1}(x_{t+1}^\tau, a)]$
10: $Q_t(\cdot, \cdot) = \min\{w_t^\top \phi(\cdot, \cdot) + \alpha[\phi(\cdot, \cdot)^\top \Lambda_t^{-1} \phi(\cdot, \cdot)]^{1/2}, T\}$
11: **end for**
12: **end for**

2.2 Optimistic LSVI

Optimistic LSVI (Jin et al., 2020) uses an optimistic Q-value with LSVI in linear MDP. We denote the feature map of the state-action pair as $\phi : \mathcal{S} \times \mathcal{A} \to \mathbb{R}^d$. The transition kernel and reward function are assumed to be linear in ϕ. Optimistic LSVI shown in Algorithm 1 consists of two parts. In the first part (line 3-6), the agent executes the policy according to Q_t for an episode. In the second part (line 7-11), the parameter w_t of Q-function is updated in closed-form by following the regularized least-squares problem

$$w_t \leftarrow \arg\min_{w \in \mathbb{R}^d} \sum\nolimits_{\tau=0}^{m} \big[r_t(s_t^\tau, a_t^\tau) + \max_{a \in \mathcal{A}} Q_{t+1}(s_{t+1}^\tau, a) - w^\top \phi(s_t^\tau, a_t^\tau)\big]^2 + \lambda \|w\|^2, \qquad (2)$$

where m is the number of episodes, and τ is the episodic index. The least-squares problem has the explicit solution $w_t = \Lambda_t^{-1} \sum_{\tau=0}^{m} \phi(x_t^\tau, a_t^\tau)\big[r_t(x_t^\tau, a_t^\tau) + \max_a Q_{t+1}(x_{t+1}^\tau, a)\big]$ (line 9), where Λ_t is the Gram matrix. Then the value function is estimated by $Q_t(s, a) \approx w_t^\top \phi(s, a)$.

Optimistic LSVI uses a bonus $\alpha[\phi(s, a)^\top \Lambda_t^{-1} \phi(s, a)]^{1/2}$ (line 10) to measure the uncertainty of state-action pairs. We can intuitively consider $u := (\phi^\top \Lambda_t^{-1} \phi)^{-1}$ as a pseudo count of state-action pair by projecting the total features that have observed (Λ_t) to the direction of the curresponding feature ϕ. Thus, the bonus $\alpha/\sqrt{u}$ represents the uncertainty along the direction of ϕ. By adding the bonus to Q-value, we obtain an optimistic value function Q^+, which serves as an upper bound of Q to encourage exploration. The bonus in each step is propagated from the end of the episode by the backward update of Q-value (line 7-11), which follows the principle of dynamic programming. Theoretical analysis (Jin et al., 2020) shows that optimistic LSVI achieves a near-optimal worst-case regret of $\tilde{\mathcal{O}}(\sqrt{d^3 T^3 L^3})$ with proper selections of α and λ, where L is the total number of steps.

3 Proposed Method

Optimistic LSVI (Jin et al., 2020) provides an atractive approach for efficient exploration. Nevertheless, developing a practical exploration algorithm for DRL is challenging, since (i) the UCB-bonus utilized by Optimistic LSVI is tailored for linear MDPs, and (ii) optimistic LSVI utilizes backward update of Q-functions (line 7-11 in Alg. 1) to aggregate uncertainty. To this end, we propose the following approaches, which are the building blocks of OEB3.

- We propose a general-purpose UCB-bonus for optimistic exploration. More specifically, we utilize bootstrapped DQN to construct a general-purpose UCB-bonus, which is theoretically consistent with optimistic LSVI for linear MDPs. We refer to Section 3.1 for the details.
- We propose a sample-efficient learning algorithm to integrate bootstrapped DQN and UCB-bonus into the backward update, which faithfully follows the principle of dynamic programming. More specifically, we extend Episodic Backward Update (EBU) (Lee et al., 2019) from ordinary Q-learning to bootstrapped Q-learning, which we abbreviate by BEBU (Bootstrapped EBU). BEBU allows sample-efficient learning and fast propagation of the future uncertainty to the estimated Q-value consistently. We further propose OEB3 by combining BEBU and the UCB-bonus obtained via bootstrapped Q-learning. We refer to Section 3.2 for the details.

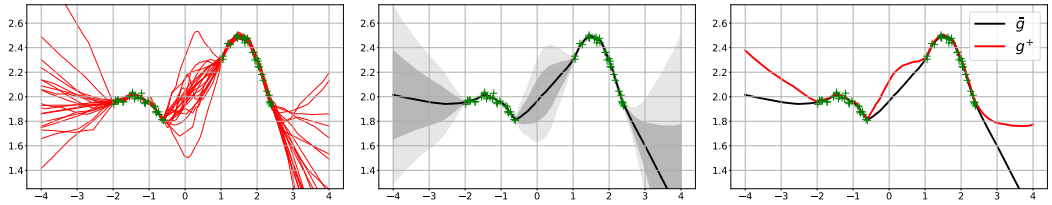

(a) (b) (c)

Figure 1: Illustration of UCB-bonus by using bootstrapped estimates in the regression task. The green dots represent 60 data points. (a) Regression curves of 20 neural networks. (b) Mean estimate (black) and uncertainty measurement (shadow). (c) The optimistic value (red) and mean value (black).

3.1 UCB-Bonus in OEB3

Optimistic exploration uses an optimistic action-value function Q^+ to incentive exploration by adding a bonus term to the ordinary Q-value. Thus Q^+ serves an upper bound of ordinary Q. The bonus term represents the epistemic uncertainty that results from lacking experiences of the corresponding states and actions. In this paper, we propose an UCB-bonus $\mathcal{B}(s_t, a_t)$ by measuring the disagreement of the bootstrapped Q-values $\{Q^k(s_t, a_t)\}_{k=1}^K$ of the state-action pair (s_t, a_t) in bootstrapped DQN, which takes the following form,

$$\mathcal{B}(s_t, a_t) := \tilde{\sigma}\big(Q^k(s_t, a_t)\big) = \sqrt{\frac{1}{K}\sum_{k=1}^{K}\Big(Q^k(s_t, a_t) - \bar{Q}(s_t, a_t)\Big)^2}, \tag{3}$$

where $\bar{Q}(s_t, a_t)$ is the mean of bootstrapped Q-values. The following theorem establishes connection between the UCB-bonus defined in Eq. (3) and the bonus in optimistic-LSVI.

Theorem 1 (Informal Version of Theorem 2)**.** *In linear function approximation, the UCB-bonus $\mathcal{B}(s_t, a_t)$ in OEB3 is equivalent to the bonus-term $[\phi_t^\top \Lambda_t^{-1} \phi_t]^{1/2}$ in optimistic-LSVI, where $\Lambda_t \leftarrow \sum_{\tau=0}^{m} \phi(x_t^\tau, a_t^\tau)\phi(x_t^\tau, a_t^\tau)^\top + \lambda \cdot \mathbf{I}$, and m is the current episode.*

We refer to Appendix A for the proof and a detailed discussion. Implementing the UCB-bonus $\mathcal{B}(s_t, a_t)$ defined in Eq. (3) in DRL is desirable for exploration for the following reasons.

- Bootstrapped DQN is a non-parametric posterior sampling method, which can be implemented via deep neural networks (Osband et al., 2019).
- The UCB-bonus $\mathcal{B}(s_t, a_t)$ defined in Eq. (3) quantifies the epistemic uncertainty of a specific state-action pair adequately. More specifically, due to the non-convexity nature of optimizing neural network and independent initialization, if (s_t, a_t) is scarcely visited, the UCB-bonus $\mathcal{B}(s_t, a_t)$ obtained via bootstrapped DQN is high. Moreover, the UCB-bonus converges to zero asymptotically as the sample size increases to infinity.
- The UCB-bonus is computed in a batch when performing experience replay, which is more efficient than other optimistic methods that change the action-selection scheme in each timestep (Chen et al., 2017; Nikolov et al., 2019).

The optimistic Q^+ is obtained by summing up the UCB-bonus and the estimated Q-function, which takes the following form,

$$Q^+(s_t, a_t) := Q(s_t, a_t) + \alpha\mathcal{B}(s_t, a_t). \tag{4}$$

We use a simple regression task with neural networks to illustrate the proposed UCB-bonus, as shown in Figure 1. We use 20 neural networks with the same network architecture to solve the same regression problem. Each network contains three residual blocks with two fully-connected layers each. According to (Osband et al., 2016), the difference between the outcome of fitting the neural networks is a result of different initialization. For a single input x, the networks yield different estimations $\{g_i(x)\}_{i=1}^{20}$ as shown in Figure 1. It follows from Figure 1(a) that the estimations $\{g_i(x)\}_{i=1}^{20}$ behave similar in the region with rich observations, resulting in small disagreement of the estimations, but vary in the region with scarce observations, resulting in large disagreement of the estimations. In Figure 1(b), we illustrate the confidence bound of the regression results $\bar{g}(x) \pm \tilde{\sigma}(g_i(x))$ and

$\bar{g}(x) \pm 2\tilde{\sigma}(g_i(x))$, where $\bar{g}(x)$ and $\tilde{\sigma}(g_i(x))$ are the mean and standard deviation of the estimations. The standard deviation $\tilde{\sigma}(g_i(x))$ captures the epistemic uncertainty of regression results. Figure 1(c) shows the optimistic estimation as $g^+(x) = \bar{g}(x) + \tilde{\sigma}(g_i(x))$ by adding the uncertainty measured by standard deviation. It can be seen that the optimistic estimation g^+ is close to $\bar{g}$ in the region with rich observations, and higher than $\bar{g}$ in the region with scarce observations.

In DRL, the bootstrapped Q-functions $\{Q^k(s_t, a_t)\}_{k=1}^K$ obtained by fitting the target Q-function perform similarly as $\{g_i(x)\}_{i=1}^{20}$ in the regression task. A higher UCB-bonus $\mathcal{B}(s_t, a_t) := \tilde{\sigma}(Q^k(s_t, a_t))$ indicates a higher epistemic uncertainty of the action-value function with (s_t, a_t). The estimated Q-function augmented with the UCB-bonus yields Q^+, which produces optimistic estimation for novel state-action pairs and behaves similar to the target Q-function in areas that are well explored by the agent. Hence, the optimistic extimation Q^+ incentives the agent to explore the potentially informative states and actions efficiently.

3.2 Bootstrapped Episodic Backward Update (BEBU)

There are two major reasons for updating the action-value function through BEBU in OEB3.

- The backward propagation utilizes a complete trajectory from the replay buffer. Such an approach allows OEB3 to infer the long-term effect of decision making from the replay buffer. In contrast, DQN and Bootstrapped DQN utilize the replay buffer by random sampling one-step transitions, which loses the information containing such a long-term effect (Lee et al., 2019).
- The backward propagation is required to propagate the future uncertainty to the estimated action-value function consistently via UCB-bonus within an episode. For instance, let $t_2 > t_1$ be the indices of two steps in an episode. If the update of Q_{t_2} occurs after the update of Q_{t_1} within an episode, then it can occur that the uncertainty propagated into Q_{t_1} is not consistent with the uncertainty that Q_{t_2} contains.

To integrate the UCB-bonus into bootstrapped Q-learning, we propose a novel Q-target in update by adding the bonus term in both the immediate reward and the next-Q value. The proposed Q-target needs to be suitable for BEBU in training. Formally, the Q-target for updating Q^k is defined as

$$y_t^k := \big[r(s_t, a_t) + \alpha_1 \mathcal{B}(s_t, a_t; \theta)\big] + \gamma\big[Q^k(s_{t+1}, a'; \theta^{k-}) + \alpha_2 \mathbb{1}_{a' \neq a_{t+1}} \tilde{\mathcal{B}}^k(s_{t+1}, a'; \theta^-)\big], \quad (5)$$

where $a' = \arg\max_a Q^k(s_{t+1}, a; \theta^{k-})$. The choice of a' is determined by the target Q-value without considering the bonus. The immediate reward is added by $\mathcal{B}(s_t, a_t; \theta)$ with a factor α_1, where the bonus $\mathcal{B}$ is computed by bootstrapped Q-network with parameter θ. The next-Q value is added by $\mathbb{1}_{a' \neq a_{t+1}} \tilde{\mathcal{B}}^k(s_{t+1}, a'; \theta^-)$ with factor α_2, where the bonus $\tilde{\mathcal{B}}^k$ is computed by the target network with parameter θ^-. We assign different bonus $\tilde{\mathcal{B}}^k$ of next-Q value to different heads, since the choice of action a' are different among the heads. Meanwhile, we assign the same bonus $\mathcal{B}$ of immediate reward for all the heads. We introduce the indicator function $\mathbb{1}_{a' \neq a_{t+1}}$ to suit the backward update of Q-values. More specifically, in the t-th step, the action-value function Q^k is updated optimistically at the state-action pair (s_{t+1}, a_{t+1}) due to the backward update. Thus, we ignore the bonus of next-Q value in the update of Q^k when a' is equal to a_{t+1}.

We use an example to explain the process of backward update. We store and sample the experiences in episodes, and perform update in episodes rather than uniformly sampled transitions. We consider an episode containing three time steps, $(s_0, a_0) \to (s_1, a_1) \to (s_2, a_2)$. We thus update the Q-value in the head k in the backward manner, namely $Q(s_2, a_2) \to Q(s_1, a_1) \to Q(s_0, a_0)$ from the end of the episode. We describe the process as follows.

1. First, we update $Q(s_2, a_2) \leftarrow r(s_2, a_2) + \alpha_1 \mathcal{B}(s_2, a_2)$. Note that in the last time step, we do not need to consider the next-Q value.
2. Then, $Q(s_1, a_1) \leftarrow [r(s_1, a_1) + \alpha_1 \mathcal{B}(s_1, a_1)] + [Q(s_2, a') + \alpha_2 \mathbb{1}_{a' \neq a_2} \tilde{\mathcal{B}}(s_2, a')]$ by following Eq. (5), where $a' = \arg\max_a Q(s_2, a)$. Since $Q(s_2, a_2)$ is updated optimistically in step 1, we ignore the bonus-term $\tilde{\mathcal{B}}$ in next-Q value when $a' = a_2$. The UCB-bonus is augmented in update by adding $\mathcal{B}$ and $\tilde{\mathcal{B}}$ to the immediate reward and next-Q value, respectively.
3. The update of $Q(s_0, a_0)$ follows the same principle. The optimistic Q-value is $Q(s_0, a_0) \leftarrow [r(s_0, a_0) + \alpha_1 \mathcal{B}(s_0, a_0)] + [Q(s_1, a') + \alpha_2 \mathbb{1}_{a' \neq a_1} \tilde{\mathcal{B}}(s_1, a')]$, where $a' = \arg\max_a Q(s_1, a)$.

In practice, the episodic update typically leads to instability in DRL due to the strong correlation in consecutive transitions. Hence, we propose a diffusion factor $\beta \in [0, 1]$ in BEBU to prevent instability as in Lee et al. (2019). The Q-value is therefore computed as the weighted sum of the current value and the back-propagated estimation scaled with factor β. We consider an episodic experience that contains T transitions, denoted by $E = \{\mathbf{S}, \mathbf{A}, \mathbf{R}, \mathbf{S}'\}$, where $\mathbf{S} = \{s_0, \dots, s_{T-1}\}$, $\mathbf{A} = \{a_0, \dots, a_{T-1}\}$, $\mathbf{R} = \{r_0, \dots, r_{T-1}\}$ and $\mathbf{S}' = \{s_1, \dots, s_T\}$. We initialize a Q-table $\tilde{\mathbf{Q}} \in \mathbb{R}^{K \times |\mathcal{A}| \times T}$ by $Q(\cdot; \theta^-)$ to store the next Q-values of all the next states $\mathbf{S}'$ and valid actions for K heads. We initialize $\mathbf{y} \in \mathbb{R}^{K \times T}$ to store the Q-target for K heads and T steps. We use bootstrapped Q-network with parameters θ to compute the bonus $\mathbf{B} = [\mathcal{B}(s_0, a_0), \dots, \mathcal{B}(s_{T-1}, a_{T-1})]$ for immediate reward, and use the target network with parameters θ^- to compute bonus $\tilde{\mathbf{B}}^k = [\tilde{\mathcal{B}}^k(s_1, a'_1), \dots, \tilde{\mathcal{B}}^k(s_T, a'_T)]$ for next-Q value in each head, where $a'_t = \arg\max_a Q^k(s_t, a; \theta^{k-})$. The bonus vector $\mathbf{B} \in \mathbb{R}^T$ is the same for all Q-heads, while $\tilde{\mathbf{B}} \in \mathbb{R}^{K \times T}$ contains different values for different heads because the choices of a'_t are different.

In the training of head k, we initialize the Q-target in the last step by $\mathbf{y}[k, T-1] = \mathbf{R}_{T-1} + \alpha_1 \mathbf{B}_{T-1}$. We then perform a recursive backward update to get all Q-target values. The elements of $\tilde{\mathbf{Q}}[k, a_{t+1}, t]$ for step t in head k is updated by using its corresponding Q-target $\mathbf{y}[k, t+1]$ with the diffusion factor as follows,

$$\tilde{\mathbf{Q}}[k, a_{t+1}, t] \leftarrow \beta \mathbf{y}[k, t+1] + (1-\beta) \tilde{\mathbf{Q}}[k, a_{t+1}, t]. \tag{6}$$

Then, we update $\mathbf{y}[k, t]$ in the previous time step based on the newly updated t-th column of $\tilde{\mathbf{Q}}[k]$ as follows,

$$\mathbf{y}[k, t] \leftarrow \big(\mathbf{R}_t + \alpha_1 \mathbf{B}_t\big) + \gamma\big(\tilde{\mathbf{Q}}[k, a', t] + \alpha_2 \mathbb{1}_{a' \neq a_{t+1}} \tilde{\mathbf{B}}[k, t]\big), \tag{7}$$

where $a' = \arg\max_a \tilde{\mathbf{Q}}[k, a, t]$. In practice, we construct a matrix $\tilde{\mathbf{A}} = \arg\max_a \tilde{\mathbf{Q}}[\cdot, a, \cdot] \in \mathbb{R}^{K \times T}$ to gather all the actions a' that correspond to the next-Q. We then construct a mask matrix $\mathbf{M} \in \mathbb{R}^{K \times T}$ to store the information whether $\tilde{\mathbf{A}}$ is identical to the executed action in the corresponding timestep or not. The bonus of next-Q is the element-wise product of $\mathbf{M}$ and $\tilde{\mathbf{B}}$ with factor α_2. After the backward update, we compute the Q-value of $(\mathbf{S}, \mathbf{A})$ as $\mathbf{Q} = Q(\mathbf{S}, \mathbf{A}; \theta) \in \mathbb{R}^{K \times T}$. The loss function takes the form of $L(\theta) = \mathbb{E}\big[(\mathbf{y} - \mathbf{Q})^2 | (s_t, a_t, r_t, s_{t+1}) \in E,\ E \sim \mathcal{D}\big]$, where the episodic experience E is sampled from replay buffer to perform gradient descent. The gradient of all heads can be computed simultaneously via BEBU. We refer the full algorithm of OEB3 to Appendix B.

We highlight that UCB-bonuses are propagated from the end of the episode along with the update of Q-functions through BEBU, which faithfully follows the backward update of optimistic LSVI in Algorithm 1 to guarantee the theoretical consistency. The backward update significantly improves the sample-efficiency by allowing bonuses and delayed rewards to propagate directly through transitions of the sampled episode, which we demonstrate in the sequel.

4 Related Work

One practical principle for exploration in DRL is maintaining epistemic uncertainty of action-value functions and learning to reduce the uncertainty. Epistemic uncertainty appears due to the missing knowledge of the environment, and disappears with the progress of exploration. Bootstrapped DQN (Osband et al., 2016; 2018) samples Q-values from the randomized value function to encourage exploration through Thompson sampling. Chen et al. (2017) shows that optimistic action-selection has better performance than randomly sampled Q-heads. Information-Directed Sampling (IDS) (Nikolov et al., 2019) is based on bootstrapped DQN, which chooses actions by balancing the instantaneous regret and information gain. OAC (Ciosek et al., 2019) uses two Q-networks to get lower and upper bounds of Q-value to perform exploration in continuous control tasks. These methods seek to estimate the epistemic uncertainty when performing action selection and choose the optimistic actions. In contrast, we use the uncertainty of value function to construct intrinsic rewards and perform backward update, which propagates future uncertainty to the estimated Q-value. Besides, our method is more time efficient, since we compute the UCB-bonus in a batch rather than in each time step. Previous methods also utilize the epistemic uncertainty of dynamics through Bayesian posterior (Ratzlaff et al., 2020) and ensembles (Pathak et al., 2019). Nevertheless, these works consider single-step uncertainty in transitions, while our method considers the long-term uncertainty in an episode.

To measure the novelty of states for constructing count-based intrinsic rewards, previous methods use density model (Bellemare et al., 2016; Ostrovski et al., 2017), static hashing (Tang et al., 2017;

Choi et al., 2019; Rashid et al., 2020), episodic curiosity (Savinov et al., 2019; Badia et al., 2020), representation changes (Raileanu & Rocktäschel, 2020), curiosity-bottleneck (Kim et al., 2019b), information gain (Houthooft et al., 2016) and random network distillation (RND) (Burda et al., 2019b). The curiosity-driven exploration based on prediction-error of environment models such as ICM (Pathak et al., 2017; Burda et al., 2019a), EMI (Kim et al., 2019a), self-aware agent (Haber et al., 2018), and learning progress (Kim et al., 2020) enable the agents to explore the environment in a self-supervised manner. According to a recent empirical research (Taiga et al., 2020), although the existing bonus-based methods show promising results in hard exploration tasks like Montezuma's Revenge, these methods do not perform well on other Atari games. Meanwhile, NoisyNet (Fortunato et al., 2018) performs significantly better than popular bonus-based methods evaluated by the whole Atari suit. Taiga et al. (2020) suggests that the real pace of progress in exploration may have been obfuscated by good results on several hard exploration games. We follow this principle and evaluate OEB3 on the whole Atari suit with 49 games.

5 Experimental Results

5.1 Environmental Setup

We evaluate the algorithms in high-dimensional image-based tasks, including Mnist Maze and 49 Atari games. We refer Appendix C for the experiments on Mnist Maze, and discuss the experiments on Atari games in the sequel. Comparing OEB3 with bootstrapped DQN-based baselines directly incur performance bias, since OEB3 uses backward update for training, which is different from bootstrapped DQN. To this end, we re-implement all bootstrapped DQN-based baselines with BEBU-based update. In our experiments, we compare the following methods: (1) **OEB3**. The proposed optimistic exploration method with UCB-bonus and backward update in this work. (2) **BEBU**. The re-implementation of bootstrapped DQN (Osband et al., 2016) with BEBU-based training. (3) **BEBU-UCB**. BEBU with optimistic action-selection according to the upper bound of Q (Chen et al., 2017). (4) **BEBU-IDS**. Integrating homoscedastic IDS (Nikolov et al., 2019) into BEBU.

According to EBU (Lee et al., 2019), the backward update is significantly more sample-efficient than ordinary Q-learning by using 20M training frames to achieve the mean human-normalized score of DQN with 200M training frames. We follow this setting by training all BEBU-based methods with 20M frames. In our experiments, 20M frames in OEB3 is sufficient to produce strong empirical results and achieve competitive results with several baselines in 200M frames. After training, an ensemble policy by a majority vote of Q-heads is used for 30 no-op evaluation (Osband et al., 2016). We use the popular human-normalized score $\frac{\text{Score}_{\text{Agent}}-\text{Score}_{\text{Random}}}{|\text{Score}_{\text{human}}-\text{Score}_{\text{random}}|}$ to perform the comparison.

We set α_1 and α_2 to the same value of 0.5×10^{-4} by searching coarsely. We use diffusion factor $\beta = 0.5$ for all methods by following Lee et al. (2019). OEB3 requires much less training time than BEBU-UCB and BEBU-IDS because the confidence bound used in BEBU-UCB and regret-information ratio used in BEBU-IDS are both computed in each time step when interacting with the environment, while the UCB-bonuses in OEB3 are calculated in episodes when performing batch training. The number of environmental interaction steps L_1 are typically set to be much larger than the number of training steps L_2 (e.g., in DQN, $L_1 \approx 4L_2$). We refer to Appendix D for the detailed specifications. The code is available at `https://bit.ly/33jv1ab`.

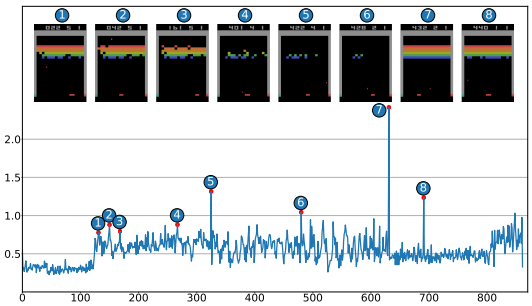

Figure 2: Visualizing UCB-bonus in Breakout

Table 1: Summary of human-normalized scores in 49 Atari games. BEBU, BEBU-UCB, BEBU-IDS and OEB3 are trained for 20M frames with RTX-2080Ti GPU for 5 random seeds.

Frames	200M				20M			
	DQN	BootDQN	NoisyNet	**BootDQN-IDS**	BEBU	BEBU-UCB	**BEBU-IDS**	**OEB3(ours)**
Mean	241%	553%	651%	**757%**	553%	610%	**622%**	**765%**
Medium	93%	139%	172%	**187%**	36%	38%	**44%**	**50%**

5.2 RESULT COMPARISON

In Table 1, we additionally report the performance of DQN (Mnih et al., 2015), NoisyNet (Fortunato et al., 2018), Bootstrapped DQN (Osband et al., 2016), and IDS (Nikolov et al., 2019) in 200M training frames. We choose NoisyNet as a baseline since it is shown (Taiga et al., 2020) to perform substantially better than existing bonus-based methods evaluated by the whole Atari suit (instead of several hard exploration games), including CTS-counts (Bellemare et al., 2016), PixelCNN-counts (Ostrovski et al., 2017), RND (Burda et al., 2019b), and ICM (Pathak et al., 2017). According to Table 1, BootDQN-IDS performs better than NoisyNet. Thus, BootDQN-IDS outperforms existing bonus-based exploration methods that perform worse than NoisyNet. We re-implement BootDQN-IDS with BEBU-based update and observe that OEB3 outperforms BEBU-IDS in both mean and medium scores, thus outperforming existing bonus-based methods that performs worse than NoisyNet. We report the raw scores in Appendix F. Moreover, Appendix G shows that OEB3 outperforms BEBU, BEBU-UCB, and BEBU-IDS in 36, 34, and 35 games out of all 49 games, respectively.

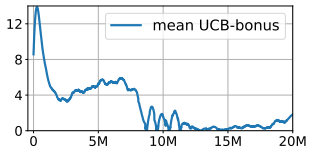

Figure 3: The change of mean UCB-bonus in Breakout

To understand the proposed UCB-bonus, we use a trained OEB3 agent to interact with the environment for an episode in Breakout and record the UCB-bonuses at each step. The curve in Figure 2 shows the UCB-bonuses of the subsampled steps in the episode. We choose 8 spikes with high UCB-bonuses and visualize the corresponding frames. The events in spikes correspond to scarcely visited areas or crucial events, which are important for the agent to obtain rewards: digging a tunnel (1), throwing the ball to the top of bricks (2,3), rebounding the ball (4,5,6), eliminating all bricks and starting a new round (7,8). We provide more examples of visualization in Appendix E. We further record the the mean of UCB-bonus of the training batch in the learning process, which is shown in Figure 3. The UCB-bonus is low at the beginning since the networks are randomly initialized. When the agent starts to explore the environment, the mean UCB-bonus rises rapidly to incentive exploration. As more experiences of states and actions are gathered, the mean UCB-bonus reduces gradually, which indicates that the bootstrapped value functions concentrate around the optimal value and the epistemic uncertainty decreases. Nevertheless, the UCB-bonuses are relatively high at scarcely visited areas or crucial events, according to Figure 2, which motivates the agent to enhance exploration at the corresponding events.

Table 2: Ablation Study

	Backward	Bonus	Qbert	SpaceInvaders	Freeway
OEB3	✓	UCB	4275.0	904.9	32.1
BootDQN-UCB	-	UCB	3284.7	731.8	20.5
BEBU	✓	-	3588.4	814.4	21.5
BootDQN	-	-	2206.8	649.5	18.3
BEBU-RND	✓	RND	3702.5	832.7	22.6

We conduct an ablation study to better comprehend the importance of backward update and bonus term in OEB3. We refer to Table 2 for the outcomes. We observe that: (1) when we use the ordinary update strategy by sampling transitions instead of episodes in training, OEB3 reduces to BootDQN-UCB with significant performance loss. Hence, the backward update is crucial in OEB3 for sample-efficient training. (2) When the UCB-bonus is set to 0, OEB3 reduces to BEBU. We observe that OEB3 outperforms BEBU in 36 out of all 49 games. (3) When both the backward update and UCB-bonus are removed, OEB3 reduces to standard BootDQN, which performs poorly in 20M training frames. (4) To illustrate the effect of UCB-bonus, we substitute UCB-bonus with the popular RND-bonus (Burda et al., 2019b). Specifically, we use an independent RND network to generate RND-bonus for each state in training. The RND-bonus is added to both the immediate reward and next-Q. The result shows that UCB-bonus outperforms RND-bonus without introducing additional modules compared to BootDQN.

6 CONCLUSION

In this work, we propose OEB3, which has theoretical underpinnings from optimistic LSVI. We propose a UCB-bonus to capture the epistemic uncertainty of Q-function and an BEBU algorithm for sample-efficient training. We demonstrate OEB3 empirically by solving Mnist maze and Atari games and show that OEB3 outperforms several strong baselines. The visualizations suggest that high UCB-bonus corresponds to informative experiences for exploration. The future directions include adapting OEB3 to continuous control and integrating OEB3 with more expressive bonus schemes.

REFERENCES

Yasin Abbasi-Yadkori, Dávid Pál, and Csaba Szepesvári. Improved algorithms for linear stochastic bandits. In *Advances in Neural Information Processing Systems*, pp. 2312–2320, 2011.

OpenAI: Marcin Andrychowicz, Bowen Baker, Maciek Chociej, Rafal Jozefowicz, Bob McGrew, Jakub Pachocki, Arthur Petron, Matthias Plappert, Glenn Powell, Alex Ray, et al. Learning dexterous in-hand manipulation. *The International Journal of Robotics Research*, 39(1):3–20, 2020.

Peter Auer and Ronald Ortner. Logarithmic online regret bounds for undiscounted reinforcement learning. In *Advances in Neural Information Processing Systems*, pp. 49–56, 2007.

Mohammad Gheshlaghi Azar, Ian Osband, and Rémi Munos. Minimax regret bounds for reinforcement learning. In *International Conference on Machine Learning*, pp. 263–272, 2017.

Adrià Puigdomènech Badia, Pablo Sprechmann, Alex Vitvitskyi, Daniel Guo, Bilal Piot, Steven Kapturowski, Olivier Tieleman, Martin Arjovsky, Alexander Pritzel, Andrew Bolt, and Charles Blundell. Never give up: Learning directed exploration strategies. In *International Conference on Learning Representations*, 2020.

Marc Bellemare, Sriram Srinivasan, Georg Ostrovski, Tom Schaul, David Saxton, and Remi Munos. Unifying count-based exploration and intrinsic motivation. In *Advances in Neural Information Processing Systems*, pp. 1471–1479, 2016.

Marc G Bellemare, Will Dabney, and Rémi Munos. A distributional perspective on reinforcement learning. In *International Conference on Machine Learning*, pp. 449–458, 2017.

Yuri Burda, Harri Edwards, Deepak Pathak, Amos Storkey, Trevor Darrell, and Alexei A Efros. Large-scale study of curiosity-driven learning. In *International Conference on Learning Representations*, 2019a.

Yuri Burda, Harrison Edwards, Amos Storkey, and Oleg Klimov. Exploration by random network distillation. In *International Conference on Learning Representations*, 2019b.

Richard Y Chen, Szymon Sidor, Pieter Abbeel, and John Schulman. Ucb exploration via q-ensembles. *arXiv preprint arXiv:1706.01502*, 2017.

Jongwook Choi, Yijie Guo, Marcin Moczulski, Junhyuk Oh, Neal Wu, Mohammad Norouzi, and Honglak Lee. Contingency-aware exploration in reinforcement learning. In *International Conference on Learning Representations*, 2019.

Kamil Ciosek, Quan Vuong, Robert Loftin, and Katja Hofmann. Better exploration with optimistic actor critic. In *Advances in Neural Information Processing Systems*, pp. 1785–1796, 2019.

Christoph Dann and Emma Brunskill. Sample complexity of episodic fixed-horizon reinforcement learning. In *Advances in Neural Information Processing Systems*, pp. 2818–2826, 2015.

Meire Fortunato, Mohammad Gheshlaghi Azar, Bilal Piot, Jacob Menick, Ian Osband, Alex Graves, Vlad Mnih, R'emi Munos, Demis Hassabis, Olivier Pietquin, Charles Blundell, and Shane Legg. Noisy networks for exploration. In *International Conference on Learning Representations*, 2018.

Scott Fujimoto, Herke Hoof, and David Meger. Addressing function approximation error in actor-critic methods. In *International Conference on Machine Learning*, pp. 1587–1596, 2018.

Nick Haber, Damian Mrowca, Stephanie Wang, Li F Fei-Fei, and Daniel L Yamins. Learning to play with intrinsically-motivated, self-aware agents. In *Advances in Neural Information Processing Systems*, pp. 8388–8399, 2018.

Rein Houthooft, Xi Chen, Yan Duan, John Schulman, Filip De Turck, and Pieter Abbeel. Vime: Variational information maximizing exploration. In *Advances in Neural Information Processing Systems*, pp. 1109–1117, 2016.

Thomas Jaksch, Ronald Ortner, and Peter Auer. Near-optimal regret bounds for reinforcement learning. *Journal of Machine Learning Research*, 11(Apr):1563–1600, 2010.

Chi Jin, Zeyuan Allen-Zhu, Sebastien Bubeck, and Michael I Jordan. Is q-learning provably efficient? In *Advances in Neural Information Processing Systems*, pp. 4863–4873, 2018.

Chi Jin, Zhuoran Yang, Zhaoran Wang, and Michael I Jordan. Provably efficient reinforcement learning with linear function approximation. In *Proceedings of Thirty Third Conference on Learning Theory*, pp. 2137–2143, 2020.

Hyoungseok Kim, Jaekyeom Kim, Yeonwoo Jeong, Sergey Levine, and Hyun Oh Song. Emi: Exploration with mutual information. In *International Conference on Machine Learning*, pp. 3360–3369, 2019a.

Kun Ho Kim, Megumi Sano, Julian De Freitas, Nick Haber, and Daniel Yamins. Active world model learning in agent-rich environments with progress curiosity. In *International Conference on Machine Learning*, 2020.

Youngjin Kim, Wontae Nam, Hyunwoo Kim, Ji-Hoon Kim, and Gunhee Kim. Curiosity-bottleneck: Exploration by distilling task-specific novelty. In *International Conference on Machine Learning*, pp. 3379–3388, 2019b.

Su Young Lee, Choi Sungik, and Sae-Young Chung. Sample-efficient deep reinforcement learning via episodic backward update. In *Advances in Neural Information Processing Systems*, pp. 2110–2119, 2019.

Marlos C Machado, Marc G Bellemare, Erik Talvitie, Joel Veness, Matthew Hausknecht, and Michael Bowling. Revisiting the arcade learning environment: Evaluation protocols and open problems for general agents. *Journal of Artificial Intelligence Research*, 61:523–562, 2018.

Volodymyr Mnih, Koray Kavukcuoglu, David Silver, Andrei A. Rusu, Joel Veness, Marc G. Bellemare, Alex Graves, Martin A. Riedmiller, Andreas Fidjeland, Georg Ostrovski, Stig Petersen, Charles Beattie, Amir Sadik, Ioannis Antonoglou, Helen King, Dharshan Kumaran, Daan Wierstra, Shane Legg, and Demis Hassabis. Human-level control through deep reinforcement learning. *Nature*, 518:529–533, 2015.

Nikolay Nikolov, Johannes Kirschner, Felix Berkenkamp, and Andreas Krause. Information-directed exploration for deep reinforcement learning. In *International Conference on Learning Representations*, 2019.

Ian Osband and Benjamin Van Roy. Why is posterior sampling better than optimism for reinforcement learning? In *International Conference on Machine Learning*, pp. 2701–2710, 2017.

Ian Osband, Charles Blundell, Alexander Pritzel, and Benjamin Van Roy. Deep exploration via bootstrapped dqn. In *Advances in neural information processing systems*, pp. 4026–4034, 2016.

Ian Osband, John Aslanides, and Albin Cassirer. Randomized prior functions for deep reinforcement learning. In *Advances in Neural Information Processing Systems*, pp. 8617–8629, 2018.

Ian Osband, Benjamin Van Roy, Daniel J Russo, and Zheng Wen. Deep exploration via randomized value functions. *Journal of Machine Learning Research*, 20(124):1–62, 2019.

Georg Ostrovski, Marc G Bellemare, Aäron van den Oord, and Rémi Munos. Count-based exploration with neural density models. In *International Conference on Machine Learning*, pp. 2721–2730, 2017.

Deepak Pathak, Pulkit Agrawal, Alexei A. Efros, and Trevor Darrell. Curiosity-driven exploration by self-supervised prediction. In *International Conference on Machine Learning*, pp. 2778–2787, 2017.

Deepak Pathak, Dhiraj Gandhi, and Abhinav Gupta. Self-supervised exploration via disagreement. In *International Conference on Machine Learning*, pp. 5062–5071, 2019.

Roberta Raileanu and Tim Rocktäschel. Ride: Rewarding impact-driven exploration for procedurally-generated environments. In *International Conference on Learning Representations*, 2020.

Tabish Rashid, Bei Peng, Wendelin Boehmer, and Shimon Whiteson. Optimistic exploration even with a pessimistic initialisation. In *International Conference on Learning Representations*, 2020.

Neale Ratzlaff, Qinxun Bai, Li Fuxin, and Wei Xu. Implicit generative modeling for efficient exploration. In *International Conference on Machine Learning*, 2020.

Daniel Russo. Worst-case regret bounds for exploration via randomized value functions. In *Advances in Neural Information Processing Systems*, pp. 14410–14420, 2019.

Nikolay Savinov, Anton Raichuk, Raphaël Marinier, Damien Vincent, Marc Pollefeys, Timothy Lillicrap, and Sylvain Gelly. Episodic curiosity through reachability. In *International Conference on Learning Representations*, 2019.

Richard S Sutton and Andrew G Barto. *Reinforcement learning: An introduction*. MIT press, 2018.

Adrien Ali Taiga, William Fedus, Marlos C Machado, Aaron Courville, and Marc G Bellemare. On bonus based exploration methods in the arcade learning environment. In *International Conference on Learning Representations*, 2020.

Haoran Tang, Rein Houthooft, Davis Foote, Adam Stooke, OpenAI Xi Chen, Yan Duan, John Schulman, Filip DeTurck, and Pieter Abbeel. Exploration: A study of count-based exploration for deep reinforcement learning. In *Advances in neural information processing systems*, pp. 2753–2762, 2017.

Mike West. Outlier models and prior distributions in bayesian linear regression. *Journal of the Royal Statistical Society: Series B (Methodological)*, 46(3):431–439, 1984.

Andrea Zanette, David Brandfonbrener, Emma Brunskill, Matteo Pirotta, and Alessandro Lazaric. Frequentist regret bounds for randomized least-squares value iteration. In *International Conference on Artificial Intelligence and Statistics*, pp. 1954–1964, 2020.

A UCB BONUS IN OEB3

Recall that we consider the following regularized least-square problem,

$$w_t \leftarrow \arg\min_{w\in\mathbb{R}^d} \sum_{\tau=0}^{m} \big[r_t(s_t^\tau, a_t^\tau) + \max_{a\in\mathcal{A}} Q_{t+1}(s_{t+1}^\tau, a) - w^\top \phi(s_t^\tau, a_t^\tau)\big]^2 + \lambda\|w\|^2. \tag{8}$$

In the sequel, we consider a Bayesian linear regression perspective of (8) that captures the intuition behind the UCB-bonus in OEB3. Our objective is to approximate the action-value function Q_t via fitting the parameter w, such that

$$w^\top \phi(s_t, a_t) \approx r_t(s_t, a_t) + \max_{a\in\mathcal{A}} Q_{t+1}(s_{t+1}, a),$$

where Q_{t+1} is given. We assume that we are given a Gaussian prior of the initial parameter $w \sim \mathcal{N}(0, \mathbf{I}/\lambda)$. With a slight abuse of notation, we denote by w_t the Bayesian posterior of the parameter w given the set of independent observations $\mathcal{D}_m = \{(s_t^\tau, a_t^\tau, s_{t+1}^\tau)\}_{\tau\in[0,m]}$. We further define the following noise with respect to the least-square problem in (8),

$$\epsilon = r_t(s_t, a_t) + \max_{a\in\mathcal{A}} Q_{t+1}(s_{t+1}, a) - w^\top \phi(s_t, a_t), \tag{9}$$

where (s_t, a_t, s_{t+1}) follows the distribution of trajectory. The following theorem justifies the UCB-bonus in OEB3 under the Bayesian linear regression perspective.

Theorem 2 (Formal Version of Theorem 1)**.** *We assume that ϵ follows the standard Gaussian distribution $\mathcal{N}(0, 1)$ given the state-action pair (s_t, a_t) and the parameter w. Let w follows the Gaussian prior $\mathcal{N}(0, \mathbf{I}/\lambda)$. We define*

$$\Lambda_t = \sum_{\tau=0}^{m} \phi(x_t^\tau, a_t^\tau)\phi(x_t^\tau, a_t^\tau)^\top + \lambda \cdot \mathbf{I}. \tag{10}$$

It then holds for the posterior of w_t given the set of independent observations $\mathcal{D}_m = \{(s_t^\tau, a_t^\tau, s_{t+1}^\tau)\}_{\tau\in[0,m]}$ that

$$\mathrm{Var}\big(\phi(s_t, a_t)^\top w_t\big) = \mathrm{Var}\big(\tilde{Q}_t(s_t, a_t)\big) = \phi(s_t, a_t)^\top \Lambda_t^{-1} \phi(s_t, a_t), \quad \forall (s_t, a_t) \in \mathcal{S}\times\mathcal{A}.$$

Here we denote by $\tilde{Q}_t = w_t^\top \phi$ the estimated action-value function.

Proof. The proof follows the standard analysis of Bayesian linear regression. See, e.g., West (1984) for a detailed analysis. We denote the target of the linear regression in (8) by

$$y_t = r_t(s_t, a_t) + \max_{a\in\mathcal{A}} Q_{t+1}(s_{t+1}, a).$$

By the assumption that ϵ follows the standard Gaussian distribution, we obtain that

$$y_t \,|\, (s_t, a_t), w \sim \mathcal{N}\big(w^\top \phi(s_t, a_t), 1\big). \tag{11}$$

Recall that we have the prior distribution $w \sim \mathcal{N}(0, \mathbf{I}/\lambda)$. Our objective is to compute the posterior density $w_t = w \,|\, \mathcal{D}_m$, where $\mathcal{D}_m = \{(s_t^\tau, a_t^\tau, s_{t+1}^\tau)\}_{\tau\in[0,m]}$ is the set of observations. It holds from Bayes rule that

$$\log p(w \,|\, \mathcal{D}_m) = \log p(w) + \log p(\mathcal{D}_m \,|\, w) + Const., \tag{12}$$

where $p(\cdot)$ denote the probability density function of the respective distributions. Plugging (11) and the probability density function of Gaussian distribution into (12) yields

$$\begin{aligned}\log p(w \,|\, \mathcal{D}_m) &= -\|w\|^2/2 - \sum_{\tau=1}^{m} \|w^\top \phi(s_t^\tau, a_t^\tau) - y_t^\tau\|^2/2 + Const. \\ &= -(w-\mu_t)^\top \Lambda_t^{-1}(w-\mu_t)/2 + Const.,\end{aligned} \tag{13}$$

where we define

$$\mu_t = \Lambda_t^{-1} \sum_{\tau=1}^{m} \phi(s_t^\tau, a_t^\tau) y_t^\tau, \qquad \Lambda_t = \sum_{\tau=0}^{m} \phi(x_t^\tau, a_t^\tau)\phi(x_t^\tau, a_t^\tau)^\top + \lambda\cdot\mathbf{I}.$$

Thus, by (13), we obtain that $w_t = w \,|\, \mathcal{D}_m \sim \mathcal{N}(\mu_t, \Lambda_t^{-1})$. It then holds for all $(s_t, a_t) \in \mathcal{S}\times\mathcal{A}$ that

$$\mathrm{Var}\big(\phi(s_t, a_t)^\top w_t\big) = \mathrm{Var}\big(\tilde{Q}_t(s_t, a_t)\big) = \phi(s_t, a_t)^\top \Lambda_t^{-1} \phi(s_t, a_t),$$

which concludes the proof of Theorem 2. □

B ALGORITHMIC DESCRIPTION

Algorithm 2 OEB3 in DRL

Initialize: replay buffer $\mathcal{D}$, bootstrapped Q-network $Q(\cdot;\theta)$ and target network $Q(\cdot;\theta^-)$
Initialize: total training frames $H = 20\text{M}$, current frame $h = 0$
while $h < H$ **do**
  Pick a bootstrapped Q-function to act by sampling $k \sim \text{Unif}\{1, \ldots, \text{K}\}$
  Reset the environment and receive the initial state s_0
  for step $i = 0$ **to** Terminal **do**
    With ϵ-greedy choose $a_i = \arg\max_a Q^k(s_i, a)$
    Take action and observe r_i and s_{i+1}, then save the transition in buffer $\mathcal{D}$
    if $h \,\%\, \text{training frequency} = 0$ **then**
      Sample an episodic experience $E = \{\mathbf{S}, \mathbf{A}, \mathbf{R}, \mathbf{S}'\}$ with length T from $\mathcal{D}$
      Initialize a Q-table $\tilde{\mathbf{Q}} = Q(\mathbf{S}', \mathcal{A}; \theta^-) \in \mathbb{R}^{K \times |\mathcal{A}| \times T}$ by the target Q-network
      Compute the UCB-bonus for immediate reward for all steps to construct $\mathbf{B} \in \mathbb{R}^T$
      Compute the action matrix $\tilde{\mathbf{A}} = \arg\max_a \tilde{\mathbf{Q}}[\cdot, a, \cdot] \in \mathbb{R}^{K \times T}$ to gather all a' of next-Q
      Compute the UCB-bonus for next-Q for all heads and all steps to construct $\tilde{\mathbf{B}} \in \mathbb{R}^{K \times T}$
      Compute the mask matrix $\mathbf{M} \in \mathbb{R}^{K \times T}$ where $\mathbf{M}[k, t] = \mathbb{1}_{\tilde{\mathbf{A}}[k,t] \neq \mathbf{A}_{t+1}}$
      Initialize target table $\mathbf{y} \in \mathbb{R}^{K \times T}$ to zeros, and set $\mathbf{y}[\cdot, T-1] = \mathbf{R}_{T-1} + \alpha_1 \mathbf{B}_{T-1}$
      for $t = T - 2$ **to** 0 **do**
        $\tilde{\mathbf{Q}}[\cdot, a_{t+1}, t] \leftarrow \beta \mathbf{y}[\cdot, t+1] + (1-\beta)\tilde{\mathbf{Q}}[\cdot, a_{t+1}, t]$
        $\mathbf{y}[\cdot, t] \leftarrow \big(\mathbf{R}_t + \alpha_1 \mathbf{B}_t\big) + \gamma\big(\tilde{\mathbf{Q}}[\cdot, a', t] + \alpha_2 \mathbf{M}[\cdot, t] \circ \tilde{\mathbf{B}}[\cdot, t]\big)$ where $a' = \tilde{\mathbf{A}}[\cdot, t]$
      end for
      Compute the Q-value of $(\mathbf{S}, \mathbf{A})$ for all heads as $\mathbf{Q} = Q(\mathbf{S}, \mathbf{A}; \theta) \in \mathbb{R}^{K \times T}$
      Perform a gradient descent step on $(\mathbf{y} - \mathbf{Q})^2$ with respect to θ
    end if
    Every C steps reset $\theta^- \leftarrow \theta$
    $h \leftarrow h + 1$
  end for
end while

C ADDITIONAL EXPERIMENT: MNIST MAZE

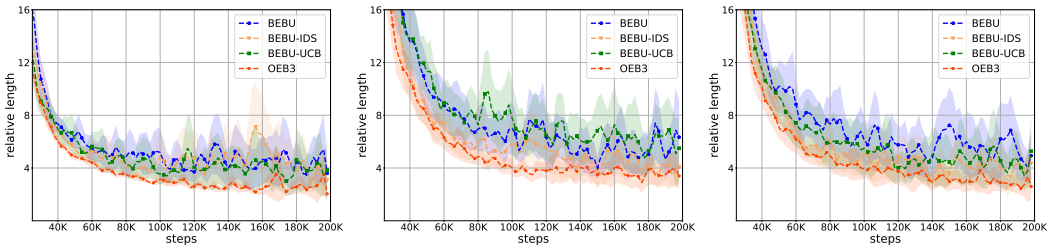

(a) Wall density of 30% (b) Wall density of 40% (c) Wall density of 50%

Figure 4: Results of 200K steps training of Mnist maze with different wall-density setup.

We use 10×10 Mnist maze with randomly placed walls to evaluate our method. The agent starts from the initial position $(0, 0)$ in the upper-left of the maze and aims to reach the goal position $(9, 9)$ in the bottom-right. The state of position (i, j) is represented by stacking two randomly sampled images with label i and j from the Mnist dataset. When the agent steps to a new position, the state representation is reconstructed by sampling images. Hence the agent gets different states even stepping to the same location twice, which minimizes the correlation among locations. We further add some stochasticity in the transition probability. The agent has a probability of 10% to arrive in the adjacent locations when taking an action. For example, when taking action 'left', the agent has a 10% chance of transiting to 'up', and a 10% chance of transiting to 'down'. The agent gets a reward of -1 when bumping into a wall, and gets 1000 when reaching the goal.

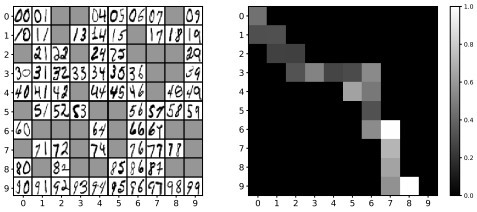

Figure 5: An example Mnist maze (left) and the UCB-bonuses in the agent's path (right).

We use the different setup of wall-density in the experiment. The wall-density means the proportion of walls in all locations. Figure 5 (left) shows a generated maze with wall-density of 50%. The gray positions represent walls. We train all methods with wall-density of 30%, 40%, and 50%. For each setup, we train 50 independent agents for 50 randomly generated mazes. The relative length defined by $l_{\text{agent}}/l_{\text{best}}$ is used to evaluate the performance, where l_{agent} is the length of the agent's path in an episode (maximum steps are 1000), and l_{best} is the length of the shortest path. The performance comparison is shown in Figure 4. OEB3 performs best in all methods, and BEBU-IDS is a strong baseline. We use a trained OEB3 agent to take action in the maze of Figure 5 (left). The UCB-bonuses of state-action pairs in the agent's path are computed and visualized in Figure 5 (right). The state-action pairs with high UCB-bonus show the bottleneck positions in the path. For example, the state-action pairs in location $(3, 3)$ and $(6, 7)$ produce high UCB-bonus to guide the agent to choose the right direction. The UCB-bonus encourages the agent to walk through these bottleneck positions correctly. We give more examples of visualization in Appendix E.

D IMPLEMENTATION DETAIL

D.1 MNIST MAZE

Hyper-parameters of BEBU. BEBU is the basic algorithm of BEBU-UCB and BEBU-IDS. BEBU uses the same network-architecture as Bootstrapped DQN (Osband et al., 2016). The diffusion factor and other training parameters are set by following EBU paper (Lee et al., 2019). Details are summarized in Table 3.

Table 3: Hyper-parameters of BEBU for Mnist-Maze

Hyperparameters	Value	Description
state space	$28 \times 28 \times 2$	Stacking two images sampled from Mnist dataset with labels according to the agent's current location.
action space	4	Including left, right, up, and down.
K	10	Number of bootstrapped heads.
network-architecture	conv(64,4,4) conv(64,3,1) dense$\{512, 4\}_{k=1}^{K}$	Using convolution (channels, kernel size, stride) layers first, then fully connected into K bootstrapped heads. Each head has 512 ReLUs and 4 linear units.
gradient norm	10	The gradient is clipped by 10. The gradient of each head is normalize by $1/K$ according to bootstrapped DQN.
learning starts	10000	The agent takes actions according to the initial policy before learning starts.
replay buffer size	170	A simple replay buffer is used to store episodic experience.
training frequency	50	Number of action-selection step between successive gradient descent steps.
H	200,000	Total timesteps to train a single maze.
target network update frequency	2000	The target-network is updated every 2000 steps.
optimizer	Adam	Adam optimizer is used for training. Detailed parameters: $\beta_1 = 0.9$, $\beta_2 = 0.999$, $\epsilon_{\text{ADAM}} = 10^{-7}$.
learning rate	0.001	Learning rate for Adam optimizer.
ϵ	$\frac{(h-H)^2}{H^2}$	Exploration factor. H is the total timesteps for training, and h is the current timestep. ϵ starts from 1 and is annealed to 0 in a quadratic manner.
γ	0.9	Discount factor.
β	1.0	Diffusion factor of backward update.
wall density	30%, 40%, and 50%	Proportion of walls in all locations of the maze.
reward	-1 or 1000	Reward is -1 when bumping into a wall, and 1000 when reaching the goal.
stochasticity	10%	Has a probability of 10% to arrive in the adjacent locations when taking an action.
evaluation metric	$l_{\text{rel}} = l_{\text{agent}}/l_{\text{best}}$	Ratio between length of the agent's path and the best length.

Hyper-parameters of BEBU-UCB. BEBU-UCB uses the upper-bound of Q-values to select actions. In particular, $a = \arg\max_{a \in \mathcal{A}} [\mu(s,a) + \lambda_{\text{ucb}}\sigma(s,a)]$, where $\mu(s,a)$ and $\sigma(s,a)$ are the mean and standard deviation of bootstrapped Q-values $\{Q^k(s,a)\}_{k=1}^{K}$. We use $\lambda_{\text{ucb}} = 0.1$ in our experiment.

Hyper-parameters of BEBU-IDS. The action-selection in IDS (Nikolov et al., 2019) follows the regret-information ratio as $a_t = \arg\min_{a \in \mathcal{A}} \frac{\hat{\Delta}_t(s,a)^2}{I_t(s,a)}$, which balances the regret and exploration. $\hat{\Delta}_t(s,a)$ is the expected regret that indicates the loss of reward when choosing a suboptimal action a. IDS uses a conservative estimate of regret as $\hat{\Delta}_t(s,a) = \max_{a' \in \mathcal{A}} u_t(s,a') - l_t(s,a)$, where $[l_t(s,a), u_t(s,a)]$ is the confidence interval of action-value function. In particular, $u_t(s,a) = \mu(s,a) + \lambda_{\text{ids}}\sigma(s,a)$ and $l_t(s,a) = \mu(s,a) - \lambda_{\text{ids}}\sigma(s,a)$, where $\mu(s,a)$ and $\sigma(s,a)$ are the mean and standard deviation of bootstrapped Q-values $\{Q^k(s,a)\}_{k=1}^{K}$. The information gain $I_t(a)$ measures the uncertainty of action-values as $I(s,a) = \log(1 + \frac{\sigma(s,a)^2}{\rho(s,a)^2}) + \epsilon_{\text{ids}}$, where $\rho(s,a)$ is the variance of the return distribution. $\rho(s,a)$ is measured by C51 (Bellemare et al., 2017) in distributional RL and becomes a constant in ordinary Q-learning. We use $\lambda_{\text{ids}} = 0.1$, $\rho(s,a) = 1.0$, and $\epsilon_{\text{ids}} = 10^{-5}$ in our experiment.

Hyper-parameters of OEB3. We set α_1 and α_2 to the same value of 0.01. We find that adding a normalizer to UCB-bonus $\tilde{\mathbf{B}}$ of the next Q-value enables us to get more stable performance. $\tilde{\mathbf{B}}$ is smoothed by dividing a running estimate of its standard deviation. Because the UCB-bonuses for next-Q are different for each Q-head, the normalization is useful in most cases by making the value function have a smooth and stable update.

D.2 ATARI GAMES

Hyper-parameters of BEBU. The basic setting of the Atari environment is the same as Nature DQN (Mnih et al., 2015) and EBU (Lee et al., 2019) papers. We use the different network architecture, environmental setup, exploration factor, and evaluation scheme from Mnist maze experiment. Details are summarized in Table 4.

Table 4: Hyper-parameters of BEBU for Atari games

Hyperparameters	Value	Description
state space	$84 \times 84 \times 4$	Stacking 4 recent frames as the input to network.
action repeat	4	Repeating each action 4 times.
K	10	The number of bootstrapped heads.
network-architecture	conv(32,8,4) conv(64,4,2) conv(64,3,1) dense$\{512, \lvert\mathcal{A}\rvert\}_{k=1}^{K}$	Using convolution(channels, kernel size, stride) layers first, then fully connected into K bootstrapped heads. Each head has 512 ReLUs and $\lvert\mathcal{A}\rvert$ linear units.
gradient norm	10	The gradient is clipped by 10, and also be normalize by $1/K$ for each head by following bootstrapped DQN.
learning starts	50000	The agent takes random actions before learning starts.
replay buffer size	1M	The number of most recent states stored in the replay buffer.
training frequency	4	The number of action-selection step between successive gradient descent steps.
H	20M	Total frames to train an environment.
target network update frequency	10000	The target-network is updated every 10000 steps.
optimizer	Adam	Adam optimizer is used for training. Detailed parameters: $\beta_1 = 0.9$, $\beta_2 = 0.999$, $\epsilon_{\mathrm{ADAM}} = 10^{-7}$.
mini-batch size	32	The number of training cases for gradient decent each time.
learning rate	0.00025	Learning rate for Adam optimizer.
initial exploration	1.0	Initial value of ϵ in ϵ-greedy exploration.
final exploration	0.1	Final value of ϵ in ϵ-greedy exploration.
final exploration frames	1M	The number of frames that the initial value of ϵ linearly annealed to the final value.
γ	0.99	Discount factor.
β	0.5	Diffusion factor of backward update.
ϵ_{eval}	0.05	Exploration factor in ϵ-greedy for evaluation.
evaluation policy	ensemble vote	The same evaluation method as in Bootstrapped DQN Osband et al. (2016).
evaluation length	108000	The policy is evaluated for 108000 steps.
evaluation frequency	100K	The policy is evaluated every 100K steps.
max no-ops	30	Maximum number no-op actions before an episode starts.

Hyper-parameters of BEBU-UCB. BEBU-UCB selects actions by $a = \arg\max_{a\in\mathcal{A}} [\mu(s,a) + \lambda_{\mathrm{ucb}}\sigma(s,a)]$. The detail is given in Appendix D.1. We use $\lambda_{\mathrm{ucb}} = 0.1$ in our experiment by searching coarsely.

Hyper-parameters of BEBU-IDS. The action-selection follows the regret-information ratio as $a_t = \arg\min_{a\in\mathcal{A}} \frac{\hat{\Delta}_t(s,a)^2}{I_t(s,a)}$. The details are given in Appendix D.1. We use $\lambda_{\mathrm{ids}} = 0.1$, $\rho(s,a) = 1.0$ and $\epsilon_{\mathrm{ids}} = 10^{-5}$ in our experiment by searching coarsely.

Hyper-parameters of OEB3. We set α_1 and α_2 to the same value of 0.5×10^{-4}. The UCB-bonus $\tilde{\mathbf{B}}$ for the next Q-value is normalized by dividing a running estimate of its standard deviation to have a stable performance.

E VISUALIZING OEB3

OEB3 uses the UCB-bonus that indicates the disagreement of bootstrapped Q-estimates to measure the uncertainty of Q-functions. The state-action pairs with high UCB-bonuses signify the bottleneck positions or meaningful events. We provide visualization in several tasks to illustrate the effect of UCB-bonuses. Specifically, we choose *Mnist-maze* and two popular Atari games *Breakout* and *Mspacman* to analyze.

E.1 MNIST-MAZE

Figure 6 illustrates the UCB-bonus in four randomly generated mazes. The mazes in Figure 6(a) and 6(b) have a wall-density of 40%, and in Figure 6(c) and 6(d) have a wall-density of 50%. The left of each figure shows the map of maze, where the black blocks represent the walls. We do not show the Mnist representation of states for simplification, and Mnist states are used in training. A trained OEB3 agent starts at the upper-left, then takes actions to achieve the goal at bottom-right. The UCB-bonuses of state-action pairs in the agent's path are computed and shown on the right of each figure. The value is normalized to $0 \sim 1$ for visualization. We show the maximal value if the agent appears several times in the same location.

The positions with UCB-bonuses that higher than 0 draw the path of the agent. The path is usually winding and includes positions beyond the shortest path because the state transition has stochasticity. The state-action pairs with high UCB-bonuses show the bottleneck positions in the path. In maze 6(a), the agent slips from the right path in position $(4, 7)$ to $(4, 9)$. The state-action in position $(4, 8)$ produces high bonus to guide the agent back to the right path. In maze 6(b), the bottleneck state in $(3, 2)$ has high bonus to avoid the agent from entering into the wrong side of the fork. The other two mazes also have bottleneck positions, like $(3, 3)$ in maze 6(c) and $(7, 6)$ in maze 6(d). Selecting actions incorrectly in these important locations is prone to failure. The UCB-bonus encourages the agent to walk through these bottleneck positions correctly.

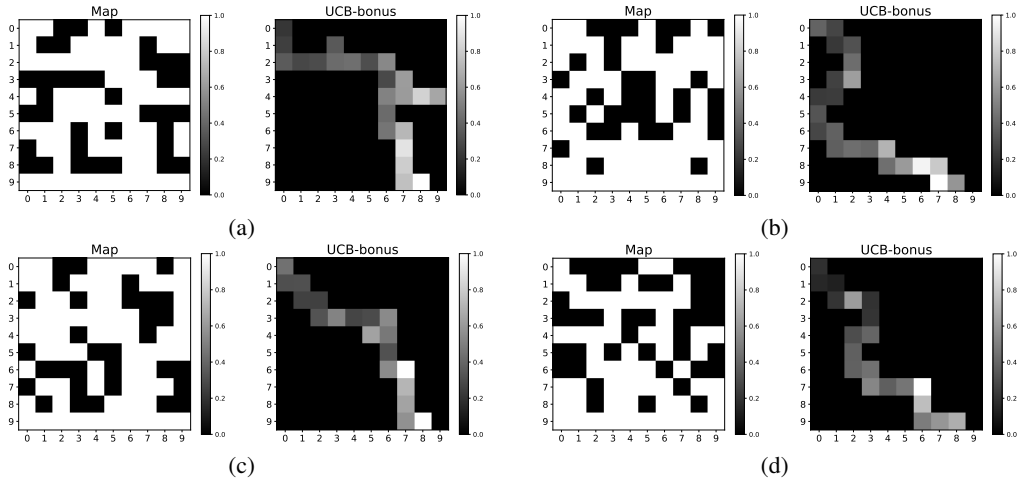

Figure 6: Visualization of UCB-bonus in Mnist-maze

E.2 BREAKOUT

In Breakout, the agent uses walls and the paddle to rebound the ball against the bricks and eliminate them. We use a trained OEB3 agent to interact with the environment for an episode in Breakout. The whole episode contains 3445 steps, and we subsample them every 4 steps for visualization. The curve in Figure 7 shows the UCB-bonus in 861 sampled steps. We choose 16 spikes with high UCB-bonuses and visualize the corresponding frames. The events in spikes usually mean meaningful experiences that are important for the agent to get rewards. In step 1, the agent is hoping to dig a tunnel and get rewards faster. After digging a tunnel, the balls appear on the top of bricks in steps 2, 3, 4, 5, 6, 9, and 12. Balls on the top are easier to hit bricks. The agents rebound the ball and throw it over the bricks in steps 7, 8, 10, and 11. In state 13, the agent eliminates all bricks and then comes to a new

round, which is novel and promising to get more rewards. The agents in steps 14, 15, and 16 rebound the ball and try to dig a tunnel again. The UCB-bonus encourages the agent to explore the potentially informative and novel state-action pairs to get high rewards. We record 15 frames after each spike for further visualization. The video is available at `https://youtu.be/VptBkHyMt8g`.

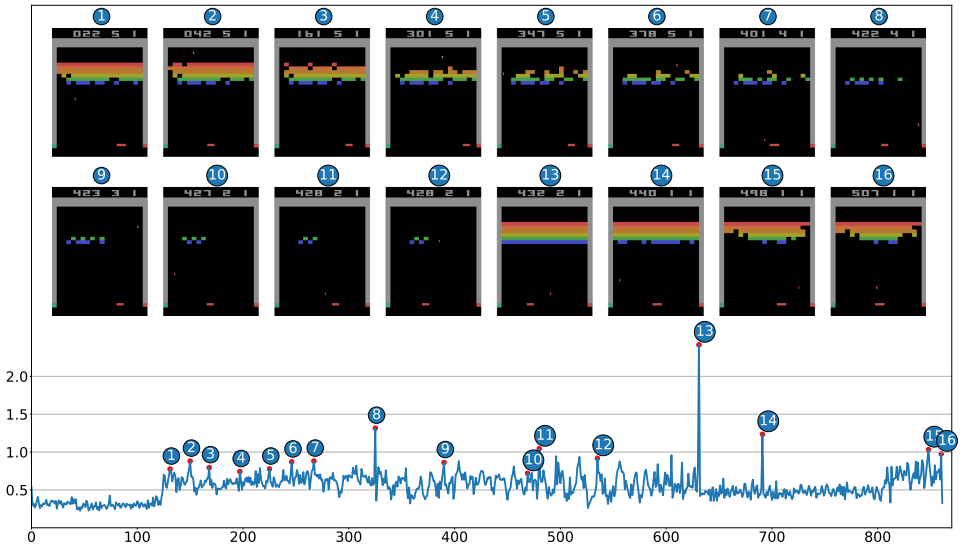

Figure 7: Visualization of UCB-bonus in Breakout

E.3 MsPacman

In MsPacman, the agent earns points by avoiding monsters and eating pellets. Eating an energizer causes the monsters to turn blue, allowing them to be eaten for extra points. We use a trained OEB3 agent to interact with the environment for an episode. Figure 8 shows the UCB bonus in all 708 steps. We choose 16 spikes to visualize the frames. The spikes of exploration bonuses correspond to meaningful events for the agent to get rewards: starting a new scenario (1,2,9,10), changing direction (3,4,13,14,16), eating energizer (5,11), eating monsters (7,8,12), and entering the corner (6,15). These state-action pairs with high UCB-bonuses make the agent explore the environment efficiently. We record 15 frames after each spike, and the video is shown at `https://youtu.be/C_8NHKpBNXM`.

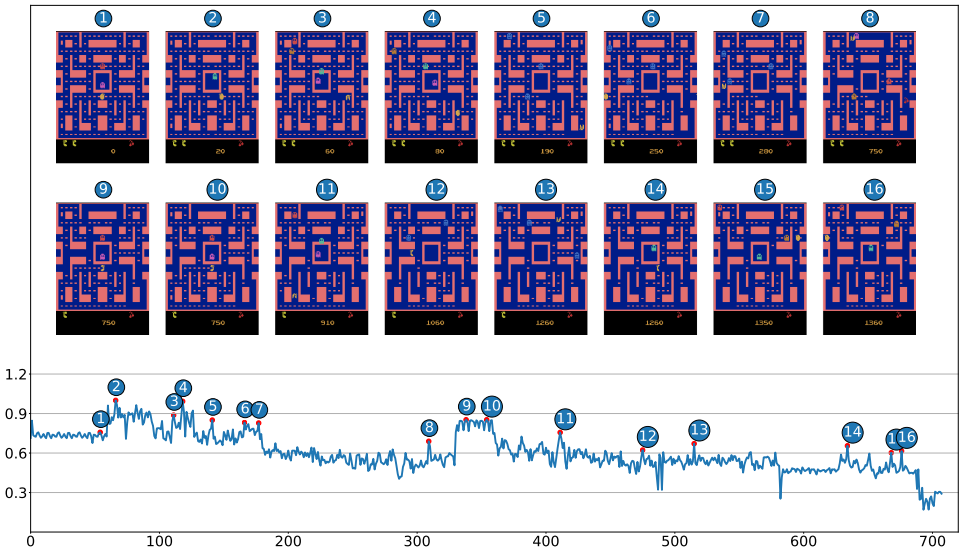

Figure 8: Visualization of UCB-bonus in MsPacman

F RAW SCORES OF ALL 49 ATARI GAMES

Table 5: Raw scores for Atari games. Each game is trained for 20M frames with a single RTX-2080Ti GPU. Bold scores signify the best score out of all methods.

	Random	Human	BEBU	BEBU-UCB	BEBU-IDS	OEB3
Alien	227.8	6,875.0	**1,118.0**	811.1	857.9	916.9
Amidar	5.8	1676.0	81.7	**166.4**	148.1	94.0
Assault	222.4	1,496.0	1,377.0	**3,574.5**	2,441.8	2,996.2
Asterix	210.0	8,503.0	2,315.0	2,709.3	2,433.9	**2,719.0**
Asteroids	719.1	13,157.0	962.8	**1,025.0**	868.8	959.9
Atlantis	12,850.0	29,028.0	3,020,500.0	3,191,600.0	3,144,440.0	**3,146,300.0**
Bank Heist	14.2	734.4	331.8	277.0	361.6	**378.6**
Battle Zone	2,360.0	37,800.0	5,446.4	**16,348.8**	10,520.0	13,454.5
BeamRider	363.9	5,775.0	2,930.0	3,208.3	3,391.0	**3,736.7**
Bowling	23.1	154.8	29.9	30.7	**40.2**	30.0
Boxing	0.1	4.3	72.4	68.3	69.8	**75.1**
Breakout	1.7	31.8	**473.2**	382.3	412.7	423.1
Centipede	2,090.9	11,963.0	2,547.2	2,377.9	**3,328.4**	2,661.8
Chopper Command	811.0	9,882.0	930.6	1,013.4	1,100.0	**1,100.3**
Crazy Climber	10,780.5	35,411.0	49,735.7	39,187.5	42,242.9	**53,346.7**
Demon Attack	152.1	3,401.0	6,506.3	6,840.4	**7,080.0**	6,794.6
Double Dunk	-18.6	-15.5	-18.9	**-16.5**	-17.0	-18.2
Enduro	0.0	309.6	504.1	697.8	513.6	**719.0**
Fishing Derby	-91.7	5.5	-56.7	-83.8	**-53.3**	-60.1
Freeway	0.0	29.6	21.5	21.6	21.3	**32.1**
Frostbite	65.2	4,335.0	393.4	470.4	466.2	**1,277.3**
Gopher	257.6	2,321.0	4,842.6	**7,211.8**	7,171.5	6,359.5
Gravitar	173.0	2,672.0	256.1	321.0	283.3	**393.6**
H.E.R.O	1,027.0	25,763.0	2,951.4	2,905.0	3,059.4	**3,302.5**
Ice Hockey	-11.2	0.9	-5.4	-6.5	-4.6	**-4.2**
Jamesbond	29.0	406.7	**650.0**	360.3	302.1	434.3
Kangaroo	52.0	3,035.0	3624.2	2,711.1	**4,448.0**	2,387.0
Krull	1,598.0	2,395.0	15,716.7	11,499.0	10,818.0	**45,388.8**
Kung-Fu Master	258.5	22,736.0	56.0	20,738.9	**26,909.7**	16,272.2
Montezuma's Revenge	0.0	4,376.0	0.0	0.0	0.0	**0.0**
Ms. Pacman	307.3	15,693.0	1,723.8	1,706.8	1,615.5	**1,794.9**
Name This Game	2,292.3	4,076.0	8,275.3	6,573.9	**8,925.0**	8,576.8
Pong	-20.7	9.3	18.1	18.5	17.2	**18.7**
Private Eye	24.9	69,571.0	1,185.8	1,925.2	1,897.1	1,174.1
Q*Bert	163.9	13,455.0	3,588.4	3,783.2	3,696.0	**4,275.0**
River Raid	1,338.5	13,513.0	3,127.5	**3,617.7**	3,169.1	2,926.5
Road Runner	11.5	7,845.0	11,483.0	20,990.7	17,281.4	**21,831.4**
Robotank	2.2	11.9	10.3	13.3	10.7	**13.5**
Seaquest	68.4	20,182.0	447.0	**492.3**	332.4	332.1
Space Invaders	148.0	1,652.0	814.4	782.2	794.7	**904.9**
Star Gunner	664.0	10,250.0	1,467.2	1,201.5	1,158.9	**1,290.2**
Tennis	-23.8	-8.9	-1.0	-2.0	-1.0	**-1.0**
Time Pilot	3,568.0	5,925.0	2,622.1	3,321.2	1,950.6	**3,404.5**
Tutankham	11.4	167.6	167.0	151.0	80.5	**297.0**
Up and Down	533.4	9,082.0	**5,954.8**	4,530.2	4,619.7	5,100.8
Venture	0.0	1,188.0	42.9	3.4	**150.0**	16.1
Video Pinball	16,256.9	17,298.0	26,829.6	48,959.1	58,398.3	**80,607.0**
Wizard of Wor	563.5	4,757.0	810.8	**1,316.7**	578.2	480.7
Zaxxon	32.5	9,173.0	1,587.5	2,104.8	1,594.2	**2,842.0**

G PERFORMANCE COMPARISON

We use the relative scores as

$$\frac{\text{Score}_{\text{Agent}} - \text{Score}_{\text{Baseline}}}{\max\{\text{Score}_{\text{human}}, \text{Score}_{\text{baseline}}\} - \text{Score}_{\text{random}}}$$

to compare OEB3 with baselines. The results of OEB3 comparing with BEBU, BEBU-UCB, and BEBU-IDS is shown in Figure 9, Figure 10, and Figure 11, respectively.

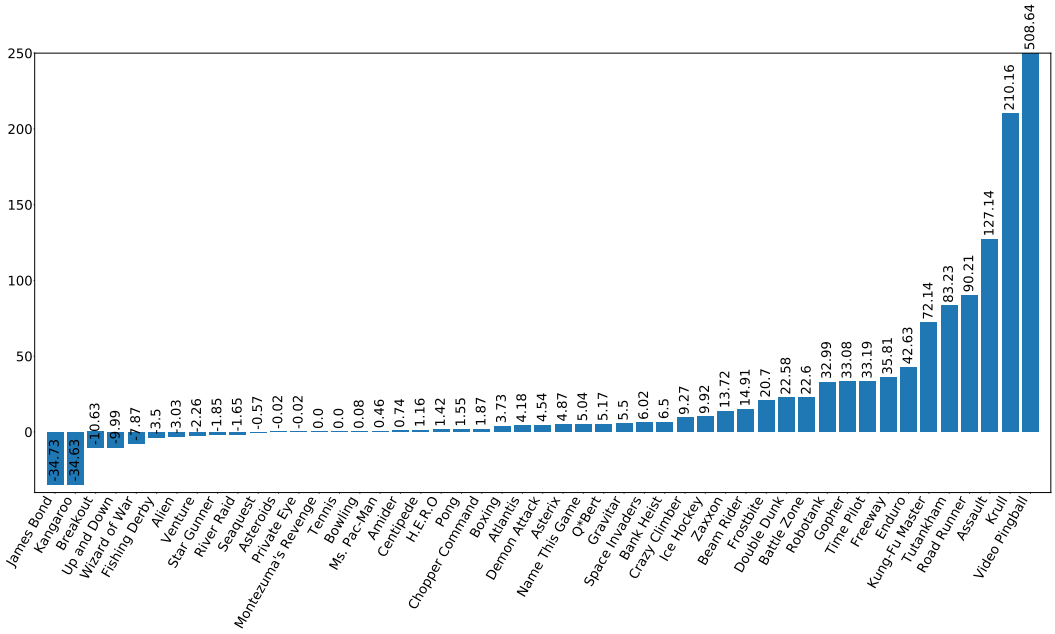

Figure 9: Relative score of OEB3 compared to BEBU in percents (%).

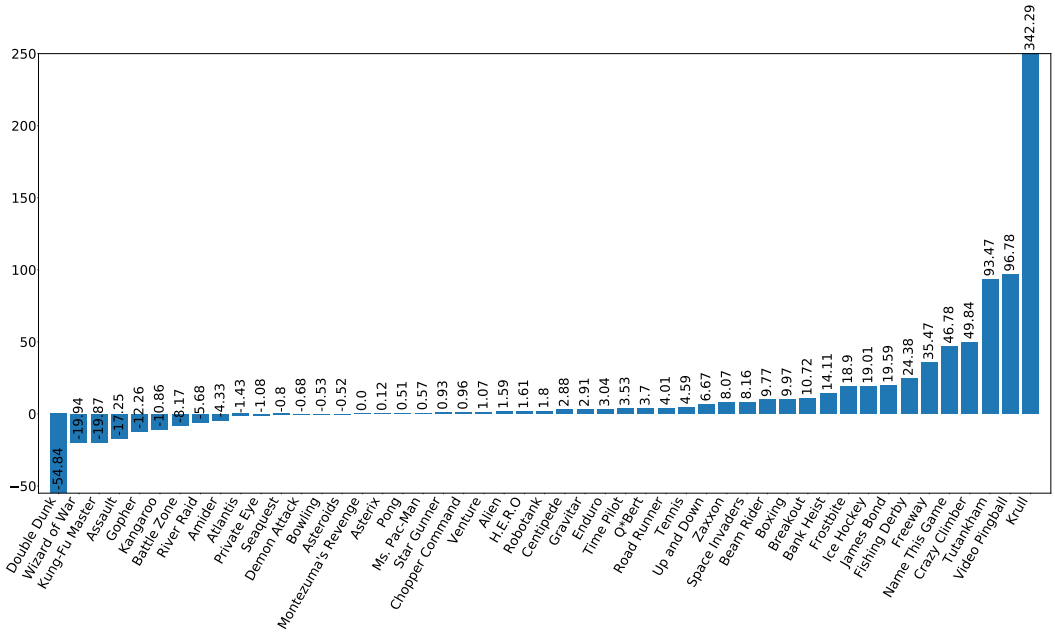

Figure 10: Relative score of OEB3 compared to BEBU-UCB in percents (%).

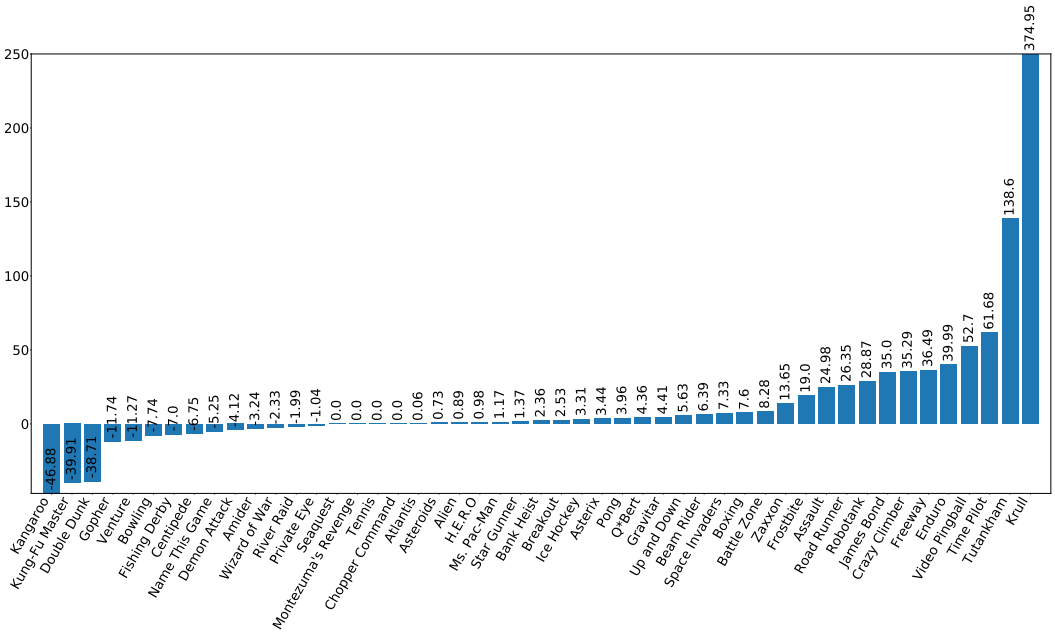

Figure 11: Relative score of OEB3 compared to BEBU-IDS in percents (%).

H Failure Analysis

Table 6: Comparison of scores in *Montezuma's Revenge.*

Frames	200M				20M			
	DQN	BootDQN	NoisyNet	BootDQN-IDS	BEBU	BEBU-UCB	BEBU-IDS	OEB3
Scores	0	100	3	0	0	0	0	0

Our method does not have a good performance on Montezuma's Revenge (see Table 6) because the epistemic uncertainty-based methods are not particularly tweaked for this domain. Bootstrapped DQN, IDS, NoisyNet and BEBU-based methods all fail in this domain and achieves no more than 100 points. In contrast, the bonus-based methods achieve significantly higher scores in this tasks (e.g., RND achieves 8152 points). However, according to Taiga et al. (2020) and Table 1, NoisyNet and IDS significantly outperforms all bonus-based methods evaluated by the whole Atari suit.